Received: 21 May 2021 | Revised: 14 September 2021 | Accepted: 30 September 2021

DOI: 10.1111/mec.16213

ORIGINAL ARTICLE

MOLECULAR ECOLOGY WILEY

Genetic diversity and the origins of parthenogenesis in the teiid lizard *Aspidoscelis laredoensis*

Anthony J. Barley[1] | James E. Cordes[2] | James M. Walker[3] | Robert C. Thomson[1]

[1]School of Life Sciences, University of Hawai'i, Honolulu, Hawai'I, USA

[2]Division of Sciences and Mathematics, Louisiana State University Eunice, Eunice, Louisiana, USA

[3]Department of Biological Sciences, University of Arkansas, Fayetteville, Arkansas, USA

Correspondence
Anthony J. Barley, School of Life Sciences, University of Hawai'i, Honolulu, Hawai'I, USA.
Email: ajbarley@hawaii.edu

Funding information
National Science Foundation, Grant/Award Number: DEB-1754350 and DEB-190017

Abstract

Unisexual vertebrates typically form through hybridization events between sexual species in which reproductive mode transitions occur in the hybrid offspring. This evolutionary history is thought to have important consequences for the ecology of unisexual lineages and their interactions with congeners in natural communities. However, these consequences have proven challenging to study owing to uncertainty about patterns of population genetic diversity in unisexual lineages. Of particular interest is resolving the contribution of historical hybridization events versus post formational mutation to patterns of genetic diversity in nature. Here we use restriction site associated DNA genotyping to evaluate genetic diversity and demographic history in *Aspidoscelis laredoensis*, a diploid unisexual lizard species from the vicinity of the Rio Grande River in southern Texas and northern Mexico. The sexual progenitor species from which one or more lineages are derived also occur in the Rio Grande Valley region, although patterns of distribution across individual sites are quite variable. Results from population genetic and phylogenetic analyses resolved the major axes of genetic variation in this species and highlight how these match predictions based on historical patterns of hybridization. We also found discordance between results of demographic modelling using different statistical approaches with the genomic data. We discuss these insights within the context of the ecological and evolutionary mechanisms that generate and maintain lineage diversity in unisexual species. As one of the most dynamic, intriguing, and geographically well investigated groups of whiptail lizards, these species hold substantial promise for future studies on the constraints of diversification in unisexual vertebrates.

KEYWORDS
demographic modelling, f-statistics, hybridization, RADseq, sex evolution, unisexual squamates

1 | INTRODUCTION

Understanding the conditions under which unisexual species evolve and are ecologically successful may help resolve the paradox of sex, one of the most fascinating and enduring questions in biology (Burke & Bonduriansky, 2017; Corley et al., 2001; Otto & Leonormand, 2002). The vast majority of vertebrates reproduce sexually, although transitions from sexual to unisexual reproduction have occurred in numerous lineages (Avise, 2008; Moreira et al., 2021). Within vertebrates, only certain species of squamates are known to reproduce entirely without the contribution of males and this form of unisexual reproduction is referred to as true parthenogenesis (Neaves & Baurmann, 2011). Although most studies of such species have focused on their evolution in nature, laboratory generation of reproductively capable unisexual lineages through hybridization has also contributed to our understanding of these phenomena (Cole et al., 2017; Lutes et al., 2011; Schultz, 1973). The success of naturally occurring unisexual lineages has long been assumed to be intimately

linked to patterns of population genetic variation, however, many different mechanisms have been invoked to explain this association and some of these make contrasting predictions.

Modes of reproduction can have profound impacts on patterns of genetic variation in natural populations. Recombination occurs in sexually reproducing species and can be positively associated with genetic diversity across a variety of scales (Case & Taper, 1986; Spencer et al., 2006). Unisexual reproduction has been predicted to lead to reduced levels of population genetic diversity. However, this relationship may often be weak due to the wide range of factors that simultaneously impact genetic variation in nature, including selection, evolutionary history, and population demography (Bengtsson, 2003; Booy et al., 2000; Ellegren & Galtier, 2016; Rabeling et al., 2011). Previous work has also shown that genetic diversity may be positively correlated with range size in unisexual lineages (Parker & Selander, 1984).

Parthenogenetic vertebrates almost exclusively evolve directly from hybridization events between sexual species, which has further consequences for patterns of genetic variation in these lineages (Barley et al., 2021a; Parker & Selander, 1976). For example, because all individuals in parthenogenetic populations (also called arrays; Walker et al., 2012) are clonally derived from F1 hybrid offspring, they usually have extremely high genome-wide levels of heterozygosity (Dessauer & Cole, 1989). This has led some authors to propose that these all-female lineages may evolve broad generalist niches as a result of heterosis, which allows them to succeed across a range of habitats (Cullum, 1997; White, 1970). By contrast, genetic variation between individuals within clonal populations is typically predicted to be low due to their reproductive mode.

Genetic variation in parthenogenetic vertebrates can be derived from two distinct processes, and these may have contrasting impacts on ecology and phenotypic variation. Most commonly, clonal populations may differ from one another as a result of novel mutations that occur following their formation through hybridization. In some squamates, this process appears to be responsible for a variety of structural mutations that have been observed in clonal populations (Cole et al., 2019; Lowe et al., 1970; Parker & Selander, 1976; Walker et al., 2012). Alternatively, independent hybridization events between the same sexual species may lead to the formation of clonal lineages that have similar ancestry, but that differ at many sites across their genome as a result of interindividual genetic variation within the parental populations (Moritz et al., 1989). Regardless of the mechanism by which it is derived, genetic diversity in clonal populations might facilitate the ecological success of parthenogenetic lineages in different ways. For example, the "general-purpose genotype" hypothesis posits that between-lineage clonal selection will promote the dominance of highly generalized genotypes with broad ecological tolerance ranges and low fitness variation (Lynch, 1984; Parker, 1979). Alternatively, the "frozen-niche variation" hypothesis suggests divergent patterns of selection may lead unisexual lineages to be composed of many genotypes with narrow ecological niches in divergent geographic regions and environments (Vrijenhoek, 1979). The importance of these phenomena in nature may also depend on how frequently new lineages form through hybridization.

Ultimately the reduced efficacy of purifying selection in clonal populations may lead to increased levels of deleterious mutational variation, which increases the likelihood of population extinction (Bast et al., 2018; Warren et al., 2018). If parthenogenetic lineages are recurrently formed through hybridization, this may drive the continual replacement of older clonal lineages with younger lineages as they form. However, similar processes may also be expected to occur under neutral models of drift (Janko, 2014; Schwander & Crespi, 2009). Despite the existence of well-developed theoretical models, our understanding of the relative importance of these different processes in nature remains limited. An important first step towards improving this understanding involves better characterizing patterns of clonal diversity in nature so that they can be compared with ecological data. Historically, clonal diversity in vertebrates has been investigated using allozyme data and histocompatibility tests (Cuellar, 1976; Neaves, 1969). For example, because histocompatible individuals must be genetically identical (or nearly so) at the highly variable major histocompatibility complex genetic loci, these tests have been used to detect parthenogenetic reproduction and distinguish single versus multiple hybridization hypotheses related to clonal diversity formation (Abuhteba et al., 2000; Cordes & Walker, 2006; Kallman, 1962; Maslin, 1967). However, both histocompatibility- and allozyme-based studies have limitations. For example, the former can be inconclusive if postformational mutations lead to histoincompatibility between populations. Genetic studies of few loci also provide limited information on the genome-wide patterns of variation that are required in order to distinguish between different demographic histories.

The most diverse clade of unisexual squamates is the North American whiptail lizards of the genus *Aspidoscelis*. One example includes *Aspidoscelis laredoensis* (Laredo Striped Whiptail), a diurnal ground-dwelling species of lizard from southern Texas and adjacent Mexico. The species is diploid, reproduces parthenogenetically, and is hypothesized to be derived from hybridization(s) between the sexual species *A. gularis* and *A. sexlineatus* based on allozyme, mitochondrial, and morphological data (Cole et al., 2020; McKinney et al., 1973; Walker et al., 2016; Wright et al., 1983). *Aspidoscelis laredoensis* occurs only in the Rio Grande Valley, typically within 10–20 km of the river (Walker et al., 2004). The association of many parthenogenetic species with disturbed habitats such as river flood plains has been thought to reflect a unique ability to colonize and exploit marginal environments (Wright & Lowe, 1968). By contrast, sexual species may be poorly adapted or competitively inferior in these types of suboptimal habitats. Two morphologically distinct clones within *A. laredoensis* have been described and referred to as clonal lineages (=clonal complexes) A and B. Histocompatibility transplants suggest these may be derived from separate historical hybridization events (Abuhteba et al., 2000, 2001). In order to better understand patterns of population genetic diversity and the ecological and evolutionary processes shaping it in this group, we used genomic data with phylogenetic and population genetic modelling to resolve their

demographic history. In doing so, we tested hypotheses regarding the number and timing of hybridization events involved in the formation of the parthenogenetic populations. We also examined the impact of these processes on genome-wide patterns of diversity in order to compare them to predictions from different theoretical models.

2 | MATERIALS AND METHODS

2.1 | Sampling and data assembly

We sampled populations of the parthenogenetic species *A. laredoensis* (Laredo Striped Whiptail), and populations of the sexual species complexes from which this species is thought to be derived: the *A. gularis* species complex and the *A. inornatus* species complex (Figure 1; Table S1). Our sampling included two phenotypically distinctive populations of *A. laredoensis*, described as A from the lower and B from the upper Rio Grande Valley (Abuhteba et al., 2000, 2001; Walker, 1987; Walker et al., 2016). We also included several samples of *A. tigris* to use as an outgroup in some analyses. We use the following acronyms for collections resources: University of Arkansas Department of Zoology (UADZ), University of Texas El Paso Biodiversity Collections (UTEP), Louisiana State University Museum of Natural Sciences (LSUH), Oklahoma Collection of Genomic Resources at the Sam Noble Museum (OCGR), American Museum of Natural History (AMNH), Museum of Vertebrate Zoology at U.C. Berkeley (MVZ), Auburn University Museum of Natural History (AUHT), California Academy of Sciences (CAS), Natural History Museum of Los Angeles County (LACM).

We genotyped each individual for ~30,000 RAD-tags using a restriction site associated DNA genotyping protocol (ddRADseq; see Barley et al., 2019 for details). All samples were sequenced as part of a larger sequencing effort on a single lane of the Illumina NovaSeq platform using a 100 base pair single end sequencing protocol. For each sample, we first estimated ploidy using nQuire (Weiß et al., 2018) to confirm all samples were diploid, as triploid individuals derived from hybridization between *A. laredoensis* and *A. gularis* have previously been documented based on morphology (Walker, 1987; Walker et al., 1991), histoincompatibility (Walker et al., 1991), karyotype, and allozyme data (Cole et al., 2020; Walker et al., 1989). The nQuire model compares distributions of variant frequencies from high throughput sequencing data to expectations under diploidy, triploidy, and tetraploidy to identify the most likely value for each sample. We used Trimmomatic (Bolger et al., 2014) to quality filter the raw sequence read data, mapped the reads to an unpublished reference genome for *A. guttatus* (sequenced with the Chromium Genome Sequencing Solution;Barley, et al., 2021b; Barley, et al., 2021a) using the BWA mem algorithm (Li & Durbin, 2010), sorted the alignments using SAMtools (Li et al., 2009), and then used the denoising implementation of nQuire to estimate ploidy based on variants with >100x coverage. We assembled the RADseq data de novo using ipyrad v0.9.26 (Eaton & Overcast, 2020) largely with default parameters. Exceptions included the clustering threshold parameter (which we determined by examining patterns of heterozygosity and missing data across a range of potential values), the

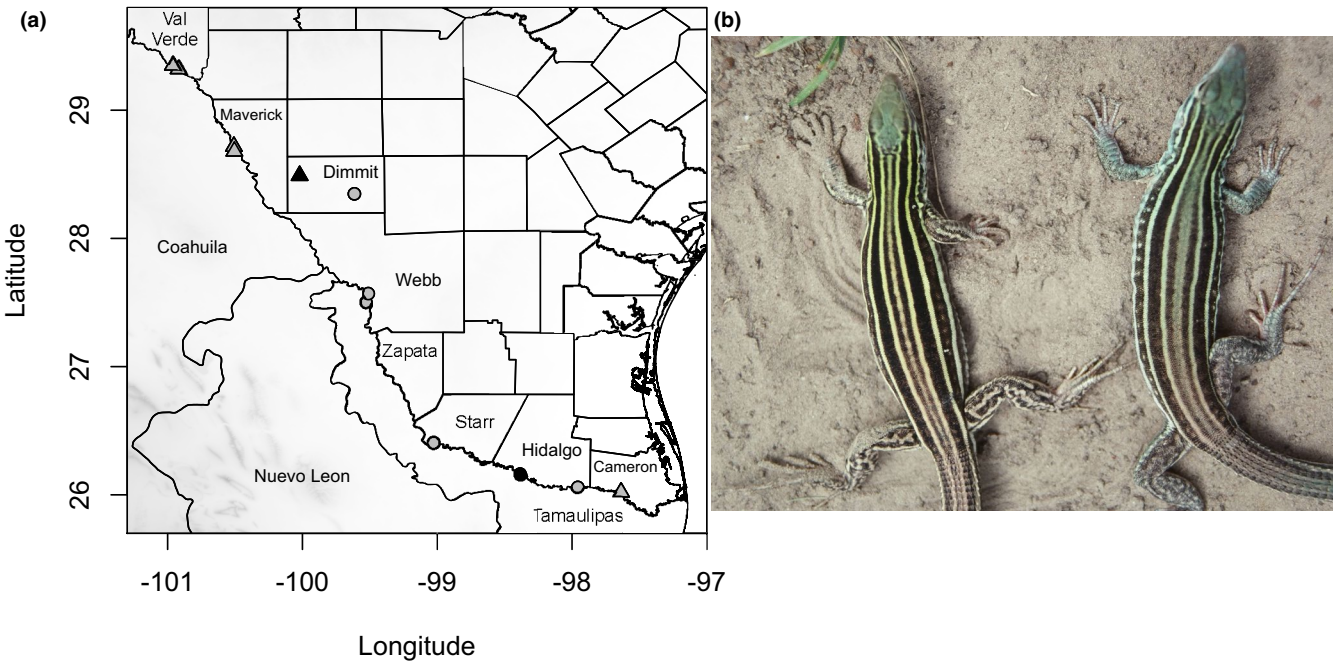

FIGURE 1 (a) Map of study area with points illustrating locality records for *Aspidoscelis laredoensis* clone A (circles) and *A. laredoensis* clone B (triangles). Grey points are records from previous studies, while black points represent sampling localities from this study. State boundaries are indicated for Mexico and county boundaries are indicated for Texas, USA. (b) Adults of *A. laredoensis* A (left) and B (right) from Bentsen Rio Grande Valley State Park, Hidalgo County, Texas (photograph by Mark A. Paulissen)

maximum proportion of shared polymorphic sites parameter (which we increased to account for the expectation that all parthenogenetic individuals are expected to share numerous heterozygous sites), and the minimum depth of coverage (filtering genotype calls with <10× coverage).

2.2 | Genetic diversity

Taxonomy and species boundaries within the two parental species complexes from which *A. laredoensis* is derived have been a subject of major historical confusion. Numerous taxa have been described within each complex based on morphology whose rank is uncertain. Species boundaries within the *A. inornatus* species complex were recently investigated by Barley et al. (2021b), Barley et al.(2021a) and we follow the recommended taxonomy from that manuscript with respect to the three primary lineages in this complex (i.e., *A. inornatus*, *A. sexlineatus*, and *A. arizonae*). A comprehensive study of species boundaries in the *A. gularis* complex is ongoing. In order to evaluate the correspondence between morphological variation and genetic variation in this group (and identify population units for analyses in this study), we evaluated the genetic relationships among populations we sampled from the *A. gularis* complex from Texas and Northern Mexico using several phylogenetic and population genetic analyses. We first performed a concatenated maximum likelihood phylogenetic analysis of the RADseq data for all the sexual species using RAxML v8.2.12 on the CIPRES Science Gateway with the GTR+Γ model and the automatic bootstrapping option. We then used the program STRUCTURE (Pritchard et al., 2000) to estimate the number of genetic clusters in the *A. gularis* data set.

We also used STRUCTURE to estimate the ancestry of *A. laredoensis* with biallelic single nucleotide polymorphism (SNP) data derived from the genomic alignments, randomly selecting a single SNP per RAD locus. We analysed two different data sets in STRUCTURE, one that included the parental species in order to estimate the hybrid ancestry of the parthenogenetic lineages, and one including only the *A. laredoensis* samples in order to identify patterns of population genetic structure within this species. For each data set analysed in STRUCTURE, we ran analyses in which we set the number of populations (K) between 1–3 and evaluated the change in likelihood across models to identify the optimal value of K. We used the admixture model in all STRUCTURE analyses and ran the MCMC for 100,000 generations following 100,000 generations of burnin. We further examined patterns of genetic relatedness by performing principal component analyses (PCA) of the SNP data using the ade4 R package (Dray & Dufour, 2007). Finally, we quantified the genetic relatedness among each of the lineages we identified in the preceding analyses using an identity-by-state (IBS) analysis with the SNPRelate package (Zheng et al., 2012) in R (v3.5.1; R Core Team, 2018). For this analysis, we pruned the data set of SNPs that were in linkage disequilibrium using the snpgdLDSpruning function with a threshold of 0.2 and performed the analysis using the snpgdsIBS function.

We estimated levels of genetic divergence (i.e., F_{ST}) between species from the SNP data using the hierfstat and SNPRelate packages in R (Zheng et al., 2012). To estimate genetic diversity within each lineage, we used the populations module in the Stacks v2.55 software. Because missing data is known to bias estimates of genetic diversity, we performed independent de novo assemblies of the RADseq data for each species. We used the default parameters in the standard Stacks modules (process_radtags, ustacks, cstacks, sstacks, tsv2bam, and gstacks) to perform the assemblies (Rochette et al., 2019). We calculated genetic diversity statistics across all sites (i.e., variant and invariant) that had no missing data in each assembly.

2.3 | Phylogenetic analyses

After identifying the major axes of genetic variation within each species/species complex we ran several phylogenetic analyses to further elucidate the evolutionary history of *A. laredoensis*. We performed a concatenated phylogenetic analysis of the RAD sequence data for the two clonal lineages of *A. laredoensis* using MrBayes v3.2.6 (Ronquist et al., 2012) to examine clonal diversity. The concatenated data set includes a single sequence per individual in which heterozygous sites are coded using standard IUPAC ambiguity codes. This analysis consisted of two Markov Chain Monte Carlo runs (for 10 million generations, sampling every 1000 generations), each with four chains, in which we used the GTR +Γ model. We estimated phylogenetic networks to resolve the hybrid ancestry of *A. laredoensis* using the unlinked biallelic SNP model implemented in the PhyloNet software (Than et al., 2008; Zhu & Nakhleh, 2018). We performed separate network analyses for clones A & B, in which we included potential ancestral populations from the *A. inornatus* and *A. gularis* species complexes. In each analysis, we limited the maximum number of reticulations to 1, allowed the population mutation rate estimates to vary across branches, and ran the analysis for 5 million MCMC iterations (sampling every 1,000 iterations following 1 million iterations of burnin).

2.4 | Demographic modelling

We also used two demographic modelling approaches to identify the best estimate of evolutionary history describing the generation of *A. laredoensis* population genetic diversity. There are two general models of primary interest (Figure S1). The first is a model in which *A. laredoensis* is derived from a single hybridization event between *A. sexlineatus* and *A. gularis*, and clones A and B formed by subsequent post formational mutation in independent populations. In the alternative model, the two clones could be derived from two independent hybridization events between *A. sexlineatus* and *A. gularis*. Demographic modelling analyses were based on SNPs extracted from the RAD-tag alignments. We performed demographic modelling with fastsimcoal2 v2.6 (Excoffier et al., 2013) using the site frequency spectrum (SFS) to test these hypotheses. We calculated

the folded SFS using easySFS (http://github.com/isaacovercast/easySFS) after identifying the optimal sample sizes for each population by downprojecting to values that maximized the number of segregating sites. We specified three demographic models under which we performed simulation, including a single origin model where clonal diversity is explained by postformational mutation following a single hybridization event. The other two analyses were performed under multiorigin models in which the two *A. laredoensis* clones were derived from independent hybridization events: one in which *A. laredoensis* A formed first and one in which *A. laredoensis* B formed first. We estimated nine parameters in the single origin model (population sizes, divergence times, and hybridization times) and eight parameters in the multiorigin models, analysed the data as site frequency spectra (FREQ option in fastimcoal2; Excoffier et al., 2013), and assumed a typical vertebrate mutation rate of $1.1e^{-8}$ (see Dryad repository for additional model details). To find the maximum likelihood parameters under each model, we performed 100 runs, each with 40 optimization cycles that consisted of 500,000 simulations. Because composite likelihoods can overestimate support when SNPs are not independent, we also obtained likelihood distributions for each model. We obtained these by performing 100 runs of 1,000,000 simulations under the maximum likelihood parameter estimates for each model. We compared the models using the distribution of Akaike information criterion (AIC) scores from these analyses. We obtained confidence intervals of the parameter estimates under each model using block-bootstrapping. We generated 100 bootstrap replicates of the SNP data set and performed parameter estimation under each model as described above to obtain confidence intervals for the parameters of interest.

Next we used admixture graphs to examine support for the different demographic models by assessing their fit to f_4 statistics calculated from the data. We used the Dsuite software (Malinsky et al., 2021) to calculate the f_4 ratios for each combination of taxa from the RADseq SNP data. For these calculations, we used the species *Aspidoscelis tigris* as an outgroup. We used the admixturegraph R package (Leppälä et al., 2017) to construct admixture graphs for the same three models that we implemented in fastsimcoal2 (described above). For each model, we used the run_metropolis_hastings function to sample the posterior distribution of model parameters for 3 million generations using six chains. Then we used the coda R package to check that each analysis had apparently converged on a stationary distribution and attained effective sample sizes (ESS) >1000. We used the model_bayes_factor_n function to calculate Bayes factors for model comparison (performing 1000 permutations to evaluate the numerical stability, mean, and standard deviation). In a more qualitative attempt to distinguish between the single origin and multiorigin models, we also examined the genome-wide distribution of F_{ST} values between clones A and B, as we expected they would differ in these two scenarios. In particular, under the single-origin model we expect most variant sites would show no differentiation between the two clones because the majority of SNP variants would have been inherited as a result of their common hybrid ancestry. A small number of loci would probably show low differentiation under this model as a result of postformational mutation in each population. In contrast, we would expect many sites from across the genome (the number of which would depend on the level of genetic diversity in the ancestral parental populations) to show high differentiation if the two clones are derived from multiple hybridization events. We calculated pairwise F_{ST} between the two clonal populations for each SNP using the Weir and Cockerham (1984) estimator in the SNPRelate package in R.

After identifying the optimal model for the evolutionary history of *A. laredoensis*, we estimated divergence times to determine the timing of formation for each clone using the multispecies-coalescent-with-introgression model implemented in BPP (Flouri et al., 2020). We fixed the topology to match the demographic history inferred above, specified diffuse, empirical priors (Campillo et al., 2020) on θ and τ in these analyses by setting $\alpha = 3$ for the inverse-gamma distributions and choosing a value for β by identifying an appropriate mean using genetic distance estimates from the RAD sequence data. We used the automatic adjustment option to finetune the proposal step lengths and ran the analysis for 1 million generations after 20,000 generations of burnin, sampling every 10 generations. We calibrated the divergence times (τ) using generation time (g) and mutation rate (μ) estimates drawn from gamma distributions using the formula: $t = \tau^*(g/\mu)$. We did this using 1000 samples of τ from the posterior distribution and constructed diffuse gamma distributions for generation time and mutation rate from which to sample in R. The gamma distribution for generation time had a mean of 1 year and a standard deviation of 0.25, whereas the mean mutation rate was set to 0.55×10^{-8} with a standard deviation of 0.225. We checked for convergence in all phylogenetic analyses using Tracer v1.7.1 (Rambaut et al., 2018) by ensuring that all parameters had reached apparent stationarity and achieved ESS's >1000.

3 | RESULTS

In total, we collected RADseq data for 27 individuals for the study, which resulted in a total of 58,172,579 reads. The mean number of reads per sample was 2,154,540 (standard deviation = 1,055,151). We used FastQC to examine read quality, which showed that all samples had uniformly high quality scores (average Phred score = 36). We combined this data with additional RADseq data from two previous studies (Table S1). Because not all sampled individuals were required for every analysis, we filtered RAD loci for each separately in order to reduce missing data and maximize power (Table S2). Analyses of the RADseq data demonstrated that all samples we phenotypically identified as *A. laredoensis* were diploid (Table 1). This included one adult individual (UADZ 9714) which we suspected might be a triploid hybrid of *A. laredoensis* x *A. gularis* based on ventral coloration, but which also appears to be diploid. Both the phylogenetic analysis and the STRUCTURE analysis of the *A. gularis* complex data set suggested there are two main genetic groups in the data (Figure S2). This result is consistent with previous taxonomic recommendations which have recognized *A. gularis* and *A. scalaris* as species, and the

Species	Catalog #	Δ 2n	Δ 3n	Δ 4n	N
laredoensis A	UADZ 9714	342.8	3149.1	1765.0	1948
laredoensis A	UADZ 9724	2540.2	8504.4	4733.3	5230
laredoensis A	UADZ 9730	1974.7	8426.5	4629.9	4681
laredoensis A	UADZ 9732	1212.4	7128.0	4277.9	4353
laredoensis A	UADZ 9734	196.5	1882.2	1060.2	1138
laredoensis A	UADZ 9735	1654.4	7591.5	4234.3	4429
laredoensis A	UADZ 9736	2499.1	8423.5	4916.2	4963
laredoensis B	UADZ 9743	1442.1	6697.2	3948.3	4099
laredoensis B	UADZ 9744	2134.9	7966.3	4507.8	4704
laredoensis B	UADZ 9745	121.4	605.1	354.2	436
laredoensis B	UADZ 9748	498.7	5609.4	3344.8	3253
laredoensis B	UADZ 9751	1238.8	6924.8	3786.5	4018

TABLE 1 Results of sample ploidy estimation using nQuire for *Aspidoscelis laredoensis* samples

Note: All samples are diploid as demonstrated by these models having the smallest change in log-likelihood compared to the free model (Δ 2n). For each sample, the number of variants genotyped at >100× coverage (N) are given.

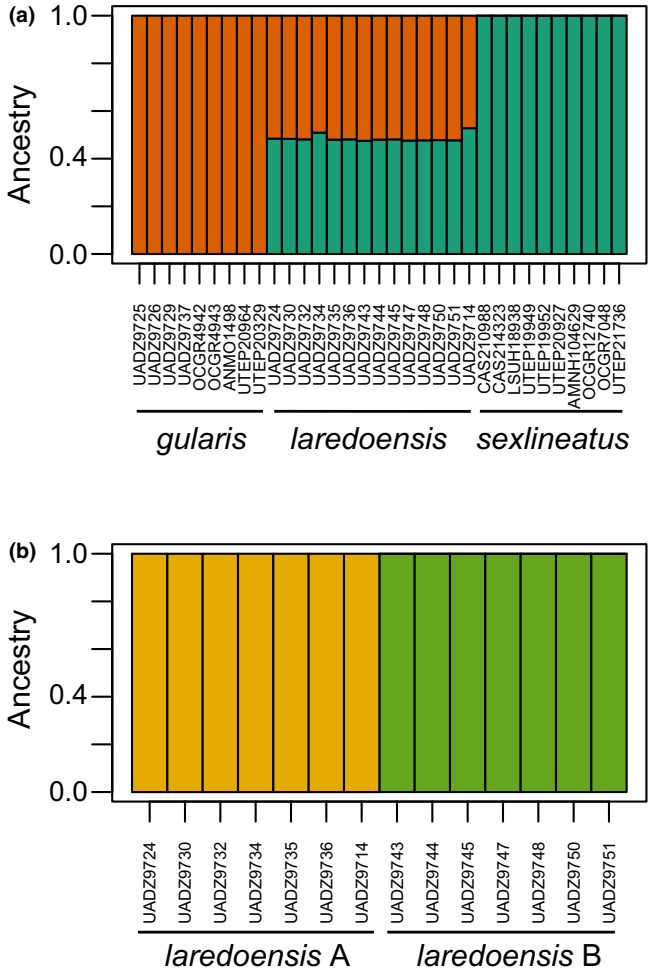

FIGURE 2 (a) Results of STRUCTURE analyses illustrating hybrid genetic ancestry of *Aspidoscelis laredoensis* compared to parental species *A. sexlineatus* and *A. gularis*. (b) STRUCTURE analysis for K = 2 illustrating genetic differentiation between two *A. laredoensis* clones

remaining taxa as subspecies. Our results suggest these subspecific taxa should be assigned to *A. scalaris* and we adopt that nomenclature here.

The STRUCTURE analyses including *A. laredoensis* identified an optimal value of 2 for K in both data sets, as the likelihood improved substantially over the analyses where K = 1, but did not in the K = 3 analyses (and the K = 2 analyses had the highest estimates for the probability of the data). For the data set including samples from the parental populations, the log-probability estimates for the data were: −498732.6 (K = 1), −337119.3 (K = 2), and −337132.9 (K = 3). For the data set including only *A. laredoensis* samples, the log-probability estimates for the data were: −54548.1 (K = 1), −30638.5 (K = 2), and −30672.8 (K = 3). These values also make biological sense. In the case of the full data set, K = 2 accounts for the two divergent sources of genetic variation derived from the sexual parental species, and the *A. laredoensis* samples were estimated as having admixed ancestry (Figure 2a). In the case of the analysis only including *A. laredoensis* samples, the analysis confirmed the presence of two distinct clones or clonal complexes, corresponding to the morphologically defined populations A and B (Figure 2b). Results of the PCA analyses also identified these two clonal populations as the major axes of genetic structure in the data sets (Figure 3), as did the phylogenetic analysis (Figure 4). Both *A. laredoensis* clones clearly have a hybrid ancestry derived from *A. sexlineatus* and *A. gularis* (Figures 2, 3, 4 Figure S3). Genetic variation within the two *A. laredoensis* clonal complexes is low, which probably reflects their relatively recent origination through hybridization, however, the two clones were clearly distinguishable based on the IBS analysis of the SNP data (Figures 3,4). Interindividual genetic variation was lower within the two clonal populations than within the two sexual species. However, interindividual genetic variation was similar in magnitude when comparing the sexual species and individuals between clones A and B (Figure 3c).

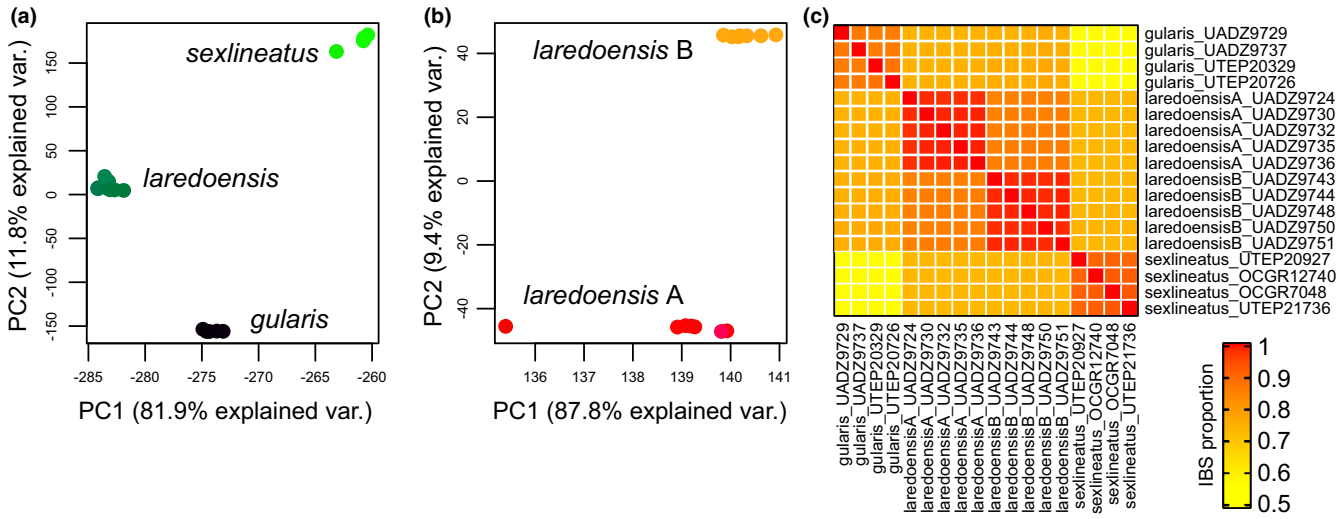

FIGURE 3 (a) Principal components analysis (PCA) illustrating major axes of genetic variation for *Aspidoscelis laredoensis* and its parental species *A. sexlineatus* and *A. gularis*. (b) PCA illustrating genetic differentiation between two *A. laredoensis* clones. (c) Heatmap from identity-by-state analysis illustrating genetic differentiation between all lineages

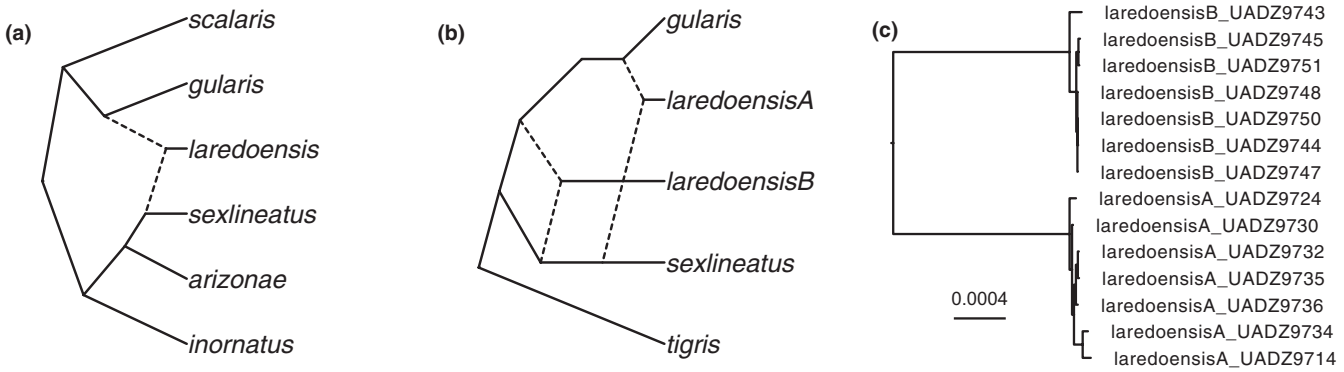

FIGURE 4 Evolutionary history of *Aspidoscelis laredoensis*. (a) Maximum a posteriori phylogenetic network from PhyloNet analysis including taxa from the two parental species complexes. All nodes in tree have posterior probability >0.95. (b) Admixture graph of the best model illustrating the formation of clones A and B. (c) 50% majority rule consensus tree from Bayesian phylogenetic analysis illustrating divergence within and between clones

TABLE 2 Results of likelihood and bayes factor (BF) model comparison using admixturegraphs showing means and standard deviations (SD)

Model	Log likelihood	Mean Loglik	Loglik SD	Mean BF	BF SD
Multiorigin B	−11431.7	−11268.8	234.5	–	–
Multiorigin A	−14620.5	−14558.8	178.1	3305.6	286.9
Single origin	−20493.4	−20358.7	619.8	9087.4	711.7

Note: Two different multiple-origin models were considered, one in which *A. laredoensis* A originated first (going forward in time) through hybridization (multiorigin A), and one in which *A. laredoensis* B be originated first (multiorigin B).

Bayes factors resulting from the fitting of admixture graphs to f_4 statistics strongly supported the multiorigin model in which clones A and B formed separately through hybridization over the single origin model in which the two clonal populations are derived from postformational mutation (Table 2). Of the two multiorigin models, the one in which clone B formed before clone A (going forward in time) was supported over the model in which clone A formed first (Table 2; Figure 4b). Interestingly, demographic modelling in fastsimcoal2 suggested that the fit between all three models for the formation of *A. laredoensis* and the data was relatively similar (although the single origin model had the largest likelihood, the distribution of AIC scores from simulation under the three models broadly overlapped; Table 3). Given the broad time interval estimates for the divergence time parameters (Figure 5), this may reflect a lack of signal in the data that would allow for more precise dating. Examination of genome-wide patterns of differentiation between clones A and B

TABLE 3 Results of model comparison using fastsimcoal2

Model	Log likelihood	AIC	AIC Distribution	T_1	T_2
Single origin	−1065944.5	4908873.9	4909708–4912172	13934–52003	1276–12307
Multi origin A	−1066379.4	4910874.4	4911813–4914628	26604–61782	30364–73624
Multi origin B	−1066394.1	4910942.1	4911107–4913369	27022–62437	29136–69903

Note: The maximum likelihood and AIC value estimates are shown for the best run, along with the distribution of AIC scores from simulation under the maximum likelihood parameters. For the single origin model, T_1 represents the time of hybridization between *A. gularis* and *A. sexlineatus* leading to the ancestral clone, while T_2 represents the time of divergence between clones A and B. For the multi origin models, the times represent the formation times through hybridization for each clone with A or B denoting the older clone in the model. Divergence time parameters are in generations, but are unscaled.

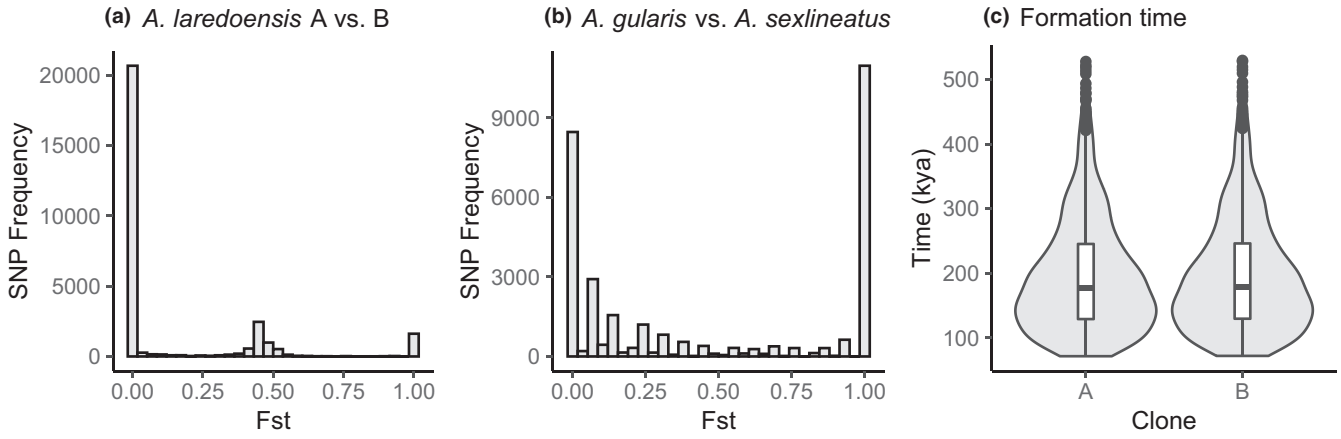

FIGURE 5 Genome-wide distribution of F_{ST} comparing *Aspidoscelis laredoensis* clone A versus clone B (a) and *A. gularis* vs. *A. sexlineatus* (b). (c) Estimate of formation time for *A. laredoensis* clones A and B based on multispecies-coalescent-with-introgression model. Violin plots illustrate probability density of divergence time estimates for the hybridization node from posterior distribution

Species	Ho	He	Π	F_{IS}
A. gularis	0.00392	0.00398	0.00428	0.00103
A. sexlineatus	0.00280	0.00444	0.00484	0.00478
A. laredoensis A	0.01033	0.00534	0.00583	−0.00828
A. laredoensis B	0.01031	0.00531	0.00580	−0.00829

TABLE 4 Observed heterozygosity (Ho), gene diversity (He), nucleotide diversity (Π), and Wright's inbreeding coefficient for each species (F_{IS})

were also consistent with our expectations under the multihybridization scenario. The SNP data show peaks of binned F_{ST} values at ~0.5 and 1.0 (Figure 5). We hypothesize that these variants correspond to sites that were variable between the two individual hybrid parents in one (0.5) or both (1.0) parental species (i.e., *A. gularis* and *A. sexlineatus*) upon hybridization. Genome-wide mean and weighted pairwise F_{ST} differentiation between the two *A. laredoensis* clones are 0.11 and 0.18, respectively. Levels of heterozygosity and gene diversity are higher in *A. laredoensis* A and B compared to *A. gularis* and *A. sexlineatus*, reflecting their hybrid ancestry, and maintenance of heterozygosity through clonal reproduction (Table 4).

4 | DISCUSSION

Here, we provide the first genome-wide assessment of clonal diversity within *A. laredoensis*. Our results confirm the presence of two major clones derived from separate, recent hybridization events between the same sexual parental lineages (*A. gularis* and *A. sexlineatus*). These genetic insights are consistent with previous morphological and biogeographic studies (Walker, 1987). Given the limited knowledge related to the mutation rate within parthenogenetic whiptails, confidence intervals for the formation times of the two clones are broad, but appear to have occurred within the past couple hundred thousand years. Both clones show similar levels of elevated heterozygosity and limited interindividual variation compared to their sexual progenitors. We also identified distinctive genomic patterns associated with their demographic history (i.e., predictable variation in genome-wide F_{ST} values between the clonal lineages). Clones A and B of *A. laredoensis* have complex, essentially parapatric distributions along the Rio Grande River in southern Texas and neighbouring northern Mexico (Walker, 1987; Walker et al., 1996). For example, along several contiguous counties in Texas, both clones A and B have been documented in some counties (Dimmit,

Hidalgo, Starr, and Webb), whereas only clone B appears to occur in Cameron, Maverick, and Val Verde (the former being widely discontinuous with the latter two), and in one county (Zapata) only clone A is known to occur. At one of our sampling sites in southern Texas (Bentsen Rio Grande Valley State Park in Hidalgo County), significant clonal turnover has been documented. In the early 1980s, clone B was overwhelmingly dominant, whereas in more recent surveys, A has become the overwhelmingly dominant form and B is rarely encountered (Walker et al., 1996). In three extended visits by JEC for our study in 2019 and 2021, sexual *A. gularis* and unisexual *A. laredoensis* A were abundant; however, no individuals of *A. laredoensis* B were observed in the park.

Given that unisexual lineages derived from multiple hybridization events will differ at many sites across the genome, this process may be conducive to the evolution of divergent ecological niches among clones and patterns that are more consistent with the "frozen-niche variation" hypothesis. This may be less likely when clonal lineages are derived from a single hybridization event and subsequent mutation that causes them to differ at only a small number of genetic loci, in which case their success might be more likely related to effects posited by the "general-purpose genotype" hypothesis. The documented pattern of clonal turnover in *A. laredoensis* is consistent with expectations if the two clones have similar ecological roles and experience strong interspecific competition in nature. The two clones have distinctive phenotypes in terms of coloration and scalation (i.e., differences in the shape, coloration, and number of the vertebral stripes and the number of granular scales that surround the body from the ventral scales on one side to the ventral scales on the opposite side; Figure 1 Walker, 1987). In contrast, they have similar neonate and adult maximum snout-vent lengths (typically to c. 28 mm SVL and 75 mm SVL, respectively). Adult sizes in both clones are intermediate compared with the parental species, and body size is often an important predictor of overlap in ecological niches between generalist insectivore lizards (Vitt, 2000). Previous ecological studies have found mixed evidence of competition between the two *A. laredoensis* clones: both show broad and flexible dietary patterns and occur in similar microhabitats, but have slight differences in activity patterns and prey preferences (Paulissen, 1994; Paulissen et al., 1988; Sievert & Paulissen, 1996). From an ecological perspective, the restriction of both *A. laredoensis* clones to a limited set of habitats in the Rio Grande Valley is inconsistent with the species having broad ecological tolerance ranges across divergent environments.

In only two areas (i.e., adjacent Webb and Dimmit counties), *A. laredoensis* occurs syntopically with both parental sexual species (Abuhteba et al., 2001; Walker et al., 2016). Some parthenogenetic arrays of whiptail lizards include triploid lineages derived from backcrossing events between diploid parthenogenetic lineages and their sexual parent species (a process referred to as "genome addition"; Barley, et al., 2021a; Wright, 1993). Although *A. laredoensis* clone A and *A. gularis* frequently hybridize (Cole et al., 2020; Walker et al., 1988), hybrids involving clone B are rare (Walker et al., 1991). The adverse factors that inhibit the existence of a triploid lineage through backcrossing events in the *A. laredoensis* complex are unknown. Of the triploid individuals derived from hybridization events between *A. laredoensis* and *A. gularis* that have been documented, one individual did appear to be parthenogenetically competent (Cole et al., 2020; Walker et al., 1991). This is the only record of a naturally occurring triploid parthenogenetic individual in this system despite substantial opportunity for their formation through hybridization. No *A. laredoensis* x *A. sexlineatus* hybrids have been documented at the few sites at which they have been found in syntopy. It is noteworthy that two recent studies by Cole et al. (2014), Cole et al. (2017) described laboratory synthesized tetraploid species from pairs of species that are widely syntopic, but have not hybridized to form new lineages in nature. They obtained *A. neavesi* through hybridization between triploid, normally parthenogenetic *A. exsanguis* x sexual *A. arizonae*, and *A. priscillae* through hybridization between triploid, normally parthenogenetic *A. uniparens* x sexual *A. arizonae*. These results indicate the potential for numerous hybrid derived species that are not realized in nature (perhaps due to ecological, behavioral, and/or other constraints). More generally, factors that determine which genetic combinations produce successful hybrid, parthenogenetic vertebrate lineages are poorly understood. However, future advances in genome sequencing may offer hope for generating insights into this subject.

4.1 | Demographic modelling

The two different demographic modelling approaches used here (i.e., the joint site frequency spectrum compared to *f*-statistics) suggested surprisingly divergent conclusions. Analyses using the former indicated there was insufficient power to distinguish between the three demographic models examined. By contrast, the latter provided strong support for the separate hybrid origin model in which the timing of formation of clone B was older. Separate hybrid origins of clones A and B are consistent with previous skin-grafting experiments, which have showed widespread histocompatibility within and histoincompatibility between the two clones (Abuhteba et al., 2000, 2001). Our examination of genome-wide patterns of F_{ST} variation was also consistent with expectations under the independent hybridization event scenario, and this may represent a straightforward, informative way to quantify hybrid clonal diversity in parthenogenetic populations.

These divergent results might have several causes. For example, down-projecting to a smaller sample size that maximizes the number of segregating sites reduces the amount of data that is used to calculate the site frequency spectrum. Model identifiability is also a concern for demographic modelling using both the SFS and *f*-statistics (Lapierre et al., 2017; Myers et al., 2008; Patterson et al., 2012; Terhorst & Song, 2015). Naively, we assumed that the joint SFS approach would perform better in distinguishing demographic models than *f*-statistics because these approaches generally utilize more information contained in the data. Admixture graphs summarize information into a single estimate of genetic distance (i.e., f_2-statistics) for each pair of populations, which might reduce the power to

distinguish among demographic histories. However, a smaller number of parameters are associated with a typical admixture graph (i.e., drift lengths and admixture weights) than SFS based models in which effective population sizes and divergence times are estimated from the data. As a consequence, SFS-based approaches typically require very large numbers of segregating sites for accurate inference. By contrast, even when an admixture graph contains nonidentifiable edges, this may not meaningfully affect the fit of the graph overall (Patterson et al., 2012). We suspect the discordance we found between these two approaches may be attributable to these differences in how the demographic models are parameterized and how the data is summarized, and that the practical outcomes of this may be underappreciated. For example, if the modelling goal is to select among simple demographic models rather than precisely estimate parameters, and a relatively small number of segregating sites are available among which linkage information is limited, this may represent a situation in which admixture modelling with *f*-statistics is more useful than SFS-based modelling.

4.2 | Ecological and evolutionary dynamics in parthenogenetic populations

The *A. laredoensis* complex represents a compelling system for studying the ecological and evolutionary dynamics of clonal turnover. For example, our demographic modelling results suggest that clone B is older (having formed first in time through hybridization). Perhaps its initial dominance at some sites (such as at Bentsen-Rio Grande Valley State Park in Hidalgo County) was facilitated by a priority effect (De Meester et al., 2016; Stroud et al., 2019). Clonal complex B not only held sway over A in 1984–1989 in this forest habitat with man-made trails, but also over maternal progenitor *A. gularis* which was rarely encountered. In the last five years of sampling, but starting much earlier (Paulissen, 1999; Walker et al., 1996), both clonal lineage A and *A. gularis* have been abundantly encountered to the near presently complete absence of clonal lineage B. Because obligately clonal lineages are expected to accumulate deleterious mutations over time, this pattern of the increasing dominance of clone A more recently would be consistent with expectations based on clonal age (e.g., if clone B became competitively inferior to clone A owing to a larger cumulative impact of Muller's Ratchet). Alternatively, and given the short time period over which these dynamics have occurred, they may be better explained by neutral processes (e.g., in which older clones decrease in frequency due to the balance of migration and drift; Janko et al., 2008). Current patterns of diversity and distribution in *A. laredoensis* provide little power with which to test predictions of the latter (neutral) models due to the limited number of extant clones, limited resolution with respect to their age, and the unknown frequency of clonal formation through hybridization in nature. However, greater genomic resources could provide evidence for a link between clonal fitness and age using the mutation frequency spectrum (i.e., differential rates of genetic decay). A combination of genomic and ecological studies would provide the greatest opportunity to elucidate process from these patterns. The *A. laredoensis* complex is probably the best group of whiptail lizards for studying these phenomena, which have long been of interest to biologists studying the evolution and maintenance of sexual systems (Schön et al., 2014).

There are six diploid parthenogenetic whiptail lineages that have distinct parental ancestry (i.e., different combinations of sexual species from which they are derived by hybridization; Wright, 1993). Only two of these lineages include multiple extant clones that have been derived from independent hybridization events. Besides *A. laredoensis*, the other example includes *A. cozumelus/A. rodecki* which are clonal lineages derived from the sexual species *A. deppii* and *A. angusticeps* that occur in the Yucatán Peninsula of southern Mexico. One of the triploid parthenogenetic whiptail lineages (which derives two copies of its genome from the sexual species *A. burti* and one from *A. arizonae*) has also been formed multiple times through hybridization. However, only one of the diploid ancestors from a primary hybridization event is known to be extant (i.e., the triploids are formed through secondary backcrosses of these diploid ancestors with sexual species; Barley, et al., 2021b; Barley, et al., 2021a). In most cases, clonal lineages of similar ancestry are understood to be allopatrically or parapatrically distributed. One exception includes *A. laredoensis* in Texas between the Gulf of Mexico (Cameron County) and Del Rio (Val Verde County) in which every conceivable distributional relationship (e.g., allopatry, parapatry, and sympatry) can be found between clones A and B. Relative abundances between clones A and B, as well as their progenitor species *A. gularis* and *A. sexlineatus* also vary widely in this region (Paulissen et al., 2001; Walker, 1987). Virtually all parthenogenetic whiptail lizards of similar genetic ancestry appear to be readily diagnosable based on traditional systematic characters that have been used in these lizards (and they were described on the basis of morphology before their separate hybrid origin was known). These patterns are consistent with genetic differences between the specific hybridizing parental individuals being important in determining the phenotypic characteristics of clonal lineages. By contrast, studies looking for evidence that parthenogenetic lineages show less interindividual variation in these types of phenotypic traits have found mixed results (Cole et al., 2016; Taylor et al., 2012).

ACKNOWLEDGEMENTS

The research was supported by grants from the National Science Foundation's Division of Environmental Biology (DEB-1754350) and Extreme Science and Engineering Discovery Environment (DEB-190017). We thank the UTEP Biodiversity Collections, the Natural History Museum of Los Angeles County, and Randy Klabacka at the Auburn University Museum of Natural History for loans of tissues samples. Tissue samples were collected by JEC in 2018 and 2019 in accordance with the provisions of Texas Parks and Wildlife (TPWD) permits SPR-1090-298, 2018-R1-5, and 2019-R1-14 issued by C. Maldonado, M. C. Jones, and N. Havlik. Partial field research funding for 2018 and 2019 was provided to JEC by an Endowed Professorship through the Louisiana

State University Eunice Foundation and Opelousas General Hospital. Additional funding for field research in 2018 and 2019 came from the Walker Family Trust. We thank Mike Hadfield and the Kewalo Marine Laboratory at the University of Hawai'i for providing access to laboratory equipment. We thank Mark Paulissen for the photograph of the two *A. laredoensis* clones.

AUTHOR CONTRIBUTIONS

James M. Walker initially proposed this project to Anthony J. Barley and all authors subsequently contributed to its conceptual development. James E. Cordes performed fieldwork to collect samples and associated data for the study. Anthony J. Barley collected and analysed the genetic data. All authors contributed to writing and editing the manuscript.

DATA AVAILABILITY STATEMENT

Demultiplexed Illumina sequence reads associated with this study have been deposited in the NCBI Sequence Read Archive (SRA PRJNA 762930). Data sets and scripts from the genetic analyses are deposited in Dryad (doi: https://doi.org/10.5061/dryad.ns1rn8ptw, Barley et al., 2021b). Contact AJB for access to the unpublished draft of the *A. guttatus* genome assembly.

ORCID

Anthony J. Barley https://orcid.org/0000-0003-1675-6577
Robert C. Thomson https://orcid.org/0000-0001-8006-1484

REFERENCES

Abuhteba, R. M., Walker, J. M., & Cordes, J. E. (2000). Genetic homogeneity based on skin histocompatibility and the evolution and systematics of parthenogenetic *Cnemidophorus laredoensis* (Sauria: Teiidae). *Canadian Journal of Zoology*, *78*, 895–904.

Abuhteba, R. M., Walker, J. M., & Cordes, J. E. (2001). Histoincompatibility between clonal complexes A and B of parthenogenetic *Cnemidophorus laredoensis*: evidence of separate hybrid origins. *Copeia*, *2001*, 262–266.

Avise, J. C. (2008). *Clonality: The genetics, ecology, and evolution of sexual abstinence in vertebrate animals*. Oxford University Press.

Barley, A. J., Cordes, J. E., Walker, J. M., & Thomson, R. C. (2021b). Data from: Genetic diversity and the origins of parthenogenesis in the teiid lizard *Aspidoscelis laredoensis*. *Dryad*, Dataset, https://doi.org/10.5061/dryad.ns1rn8ptw

Barley, A. J., Nieto-Montes de Oca, A., Reeder, T. W., Manríquez-Morán, N. L., Arenas Monroy, J. C., Hernández-Gallegos, O., & Thomson, R. C. (2019). Complex patterns of hybridization and introgression across evolutionary timescales in Mexican whiptail lizards (*Aspidoscelis*). *Molecular Phylogenetics and Evolution*, *132*, 284–295. https://doi.org/10.1016/j.ympev.2018.12.016

Barley, A. J., Reeder, T. W., Nieto-Montes de Oca, A., Cole, C. J., & Thomson, R. C. (2021a). A new diploid parthenogenetic whiptail lizard from Sonora, Mexico is the predicted 'missing link' in the evolutionary transition to polyploidy. *The American Naturalist*, *198*, 295–309.

Bast, J., Parker, D. J., Dumas, Z., Jalvingh, K. M., Van, P. T., Jaron, K. S., Figuet, E., Brandt, A., Galtier, N., & Schwander, T. (2018). Consequences of asexuality in natural populations: Insights from stick insects. *Molecular Biology and Evolution*, *35*, 1668–1677. https://doi.org/10.1093/molbev/msy058

Bengtsson, B. O. (2003). Genetic variation in organisms with sexual and asexual reproduction. *Journal of Evolutionary Biology*, *16*, 189–199. https://doi.org/10.1046/j.1420-9101.2003.00523.x

Bolger, A. M., Lohse, M., & Usadel, B. (2014). Trimmomatic: A flexible trimmer for Illumina sequence data. *Bioinformatics*, *30*, 2114–2120. https://doi.org/10.1093/bioinformatics/btu170

Booy, G., Hendriks, R. J. J., Smulders, M. J. M., Groenendael, J. M., & Vosman, B. (2000). Genetic diversity and the survival of populations. *Plant Biology*, *2*, 379–395. https://doi.org/10.1055/s-2000-5958

Burke, N. W., & Bonduriansky, R. (2017). Sexual conflict, facultative asexuality, and the true paradox of sex. *Trends in Ecology and Evolution*, *32*, 646–652. https://doi.org/10.1016/j.tree.2017.06.002

Campillo, L. C., Barley, A. J., & Thomson, R. C. (2020). Model-based species delimitation: Are coalescent species reproductively isolated? *Systematic Biology*, *69*, 708–721. https://doi.org/10.1093/sysbio/syz072

Case, T. J., & Taper, M. L. (1986). On the coexistence and coevolution of asexual and sexual competitors. *Evolution*, *40*, 366–387. https://doi.org/10.1111/j.1558-5646.1986.tb00478.x

Cole, C. J., Cordes, J. E., & Walker, J. M. (2019). Karyotypes of the North American parthenogenetic whiptail lizard *Aspidoscelis velox*, and return of *Aspidoscelis innotatus* to the synonymy of *A. velox* (Reptilia: Squamata: Teiidae). *American Museum Novitates*, *3936*, 1–8. https://doi.org/10.1206/3936.1

Cole, C. J., Dessauer, H. C., Paulissen, M. A., & Walker, J. M. (2020). Hybridization between whiptail lizards in Texas: *Aspidoscelis laredoensis* and *A. gularis*, with notes on reproduction of a hybrid. *American Museum Novitates*, *2020*, 1–13. https://doi.org/10.1206/3947.1

Cole, C. J., Taylor, H. L., Baumann, D. P., & Baumann, P. (2014). Neaves' whiptail lizard: The first known tetraploid parthenogenetic tetrapod (Reptilia: Squamata: Teiidae). *Breviora*, *539*, 1–20. https://doi.org/10.3099/MCZ17.1

Cole, C. J., Taylor, H. L., Neaves, W. B., Baumann, D. P., Newton, A., Schnittker, R., & Baumann, P. (2017). The second known tetraploid species of parthenogenetic tetrapod (Reptilia: Squamata: Teiidae): Description, reproduction, comparisons with ancestral taxa, and origins of multiple clones. *Bulletin of the Museum of Comparative Zoology*, *161*, 285–321. https://doi.org/10.3099/MCZ37.1

Cole, C. J., Taylor, H. L., & Townsend, C. R. (2016). Morphological variation in a unisexual whiptail lizard (*Aspidoscelis exsanguis*) and one of its bisexual parental species (*Aspidoscelis inornata*) (Reptilia: Squamata: Teiidae): Is the clonal species less variable? *American Museum Novitates*, *3849*, 1–20.

Cordes, J. E., & Walker, J. M. (2006). Evolutionary and systematic implications of skin histocompatibility among parthenogenetic teiid lizards: three color pattern classes of *Aspidoscelis dixoni* and one of *Aspidoscelis tesselata*. *Copeia*, *2006*, 14–26.

Corley, L. S., Blankenship, J. R., & Moore, A. J. (2001). Genetic variation and asexual reproduction in the facultatively parthenogenetic cockroach *Nauphoeta cinerea*: Implications for the evolution of sex. *Journal of Evolutionary Biology*, *14*, 68–74.

Cuellar, O. (1976). Intraclonal histocompatibility in a parthenogenetic lizard: Evidence of genetic homogeneity. *Science*, *193*, 150–153. https://doi.org/10.1126/science.779030

Cullum, A. J. (1997). Comparisons of physiological performance in sexual and asexual whiptail lizards (genus *Cnemidophorus*): Implications for the role of heterozygosity. *The American Naturalist*, *150*, 24–47.

De Meester, L., Vanoverbeke, J., Kilsdonk, L. J., & Urban, M. C. (2016). Evolving perspectives on monopolization and priority effects. *Trends in Ecology and Evolution*, *31*, 136–146. https://doi.org/10.1016/j.tree.2015.12.009

Dessauer, H. C., & Cole, C. J. (1989). Diversity between and within nominal forms of unisexual teiid lizards. *Evolution and ecology of unisexual vertebrates* (pp. 49–71). New York State Museum Bulletin.

Dray, S., & Dufour, A. B. (2007). The ade4 package: Implementing the duality diagram for ecologists. *Journal of Statistical Software*, *22*, 1–20.

Eaton, D. A. R., & Overcast, I. (2020). ipyrad: Interactive assembly and analysis of RADseq datasets. *Bioinformatics*, *36*, 2592–2594.

Ellegren, H., & Galtier, N. (2016). Determinants of genetic diversity. *Nature Reviews Genetics*, *17*, 422–433. https://doi.org/10.1038/nrg.2016.58

Excoffier, L., Dupanloup, I., Huerta-Sánchez, E., Sousa, V. C., & Foll, M. (2013). Robust demographic inference from genomic and SNP data. *PLoS Genetics*, *9*, e1003905. https://doi.org/10.1371/journal.pgen.1003905

Flouri, T., Jiao, X., Rannala, B., & Yang, Z. (2020). A Bayesian implementation of the multispecies coalescent model with introgression for phylogenomic analysis. *Molecular Biology and Evolution*, *37*, 1211–1223. https://doi.org/10.1093/molbev/msz296

Janko, K. (2014). Let us not be unfair to asexuals: their ephemerality may be explained by neutral models without invoking any evolutionary constraints of asexuality. *Evolution*, *68*, 569–576. https://doi.org/10.1111/evo.12293

Janko, K., Drozd, P., Flegr, J., & Pannell, J. R. (2008). Clonal turnover versus clonal decay: A null model for observed patterns of asexual longevity, diversity and distribution. *Evolution*, *62*, 1264–1270. https://doi.org/10.1111/j.1558-5646.2008.00359.x

Kallman, K. D. (1962). Gynogenesis in the teleost, *Mollienesia formosa* (Girard), with a discussion of the detection of parthenogenesis in vertebrates by tissue transplantation. *Journal of Genetics*, *58*, 7–24. https://doi.org/10.1007/BF02986114

Lapierre, M., Lambert, A., & Achaz, G. (2017). Accuracy of demographic inferences from the site frequency spectrum: The case of the Yoruba population. *Genetics*, *206*, 139–449. https://doi.org/10.1534/genetics.116.192708

Leppälä, K., Nielsen, S. V., & Mailund, T. (2017). admixturegraph: An R package for admixture graph manipulation and fitting. *Bioinformatics*, *33*, 1738–1740. https://doi.org/10.1093/bioinformatics/btx048

Li, H., & Durbin, R. (2010). Fast and accurate long-read alignment with Burrows-Wheeler transform. *Bioinformatics*, *26*, 589–595. https://doi.org/10.1093/bioinformatics/btp698

Li, H., Handsaker, B., Wysoker, A., Fennell, T., Ruan, J., Homer, N., Marth, G., Abecasis, G., & Durbin, R.; 1000 Genome Project Data Processing Subgroup. (2009). The sequence alignment/map format and SAMtools. *Bioinformatics*, *25*, 2078–2079. https://doi.org/10.1093/bioinformatics/btp352

Lowe, C. H., Wright, J. W., Cole, C. J., & Bezy, R. L. (1970). Natural hybridization between the Teiid lizards *Cnemidophorus sonorae* (parthenogenetic) and *Cnemidophorus tigris* (bisexual). *Systematic Zoology*, *19*, 114.

Lutes, A. A., Baumann, D. P., Neaves, W. B., & Baumann, P. (2011). Laboratory synthesis of an independently reproducing vertebrate species. *Proceedings of the National Academy of Sciences of the United States of America*, *108*, 9910–9915. https://doi.org/10.1073/pnas.1102811108

Lynch, M. (1984). Destabilizing hybridization, general-purpose genotypes and geographic parthenogenesis. *The Quarterly Review of Biology*, *59*, 257–290. https://doi.org/10.1086/413902

Malinsky, M., Matschiner, M., & Svardal, H. (2021). Dsuite - Fast *D*-statistics and related admixture evidence from VCF files. *Molecular Ecology Resources*, *21*, 584–595.

Maslin, T. P. (1967). Skin grafting in the bisexual teiid lizard *Cnemidophorus sexlineatus* and in the unisexual *C. tesselatus*. *Journal of Experimental Zoology*, *166*, 137–149. https://doi.org/10.1002/jez.1401660114

McKinney, C. O., Kay, F. R., & Anderson, R. A. (1973). A new all-female species of the genus *Cnemidophorus*. *Herpetologica*, *29*, 361–366.

Moreira, M. O., Fonseca, C., & Rojas, D. (2021). Parthenogenesis is self-destructive for scaled reptiles. *Biology Letters*, *17*, rsbl.2021.0006. https://doi.org/10.1098/rsbl.2021.0006

Moritz, C., Brown, W. M., Densmore, L. D., Wright, J. W., Vyas, D., Donellan, S., Adams, M., & Baverstock, P. (1989). Genetic diversity and the dynamics of hybrid parthenogenesis in *Cnemidophorus* (Teiidae) and *Heteronotia* (Gekkonidae). *Evolution and ecology of unisexual vertebrates* (pp. 87–112). New York State Museum.

Myers, S., Fefferman, C., & Patterson, N. (2008). Can one learn history from the allelic spectrum? *Theoretical Population Biology*, *73*, 342–348. https://doi.org/10.1016/j.tpb.2008.01.001

Neaves, W. B. (1969). Adenosine deaminase phenotypes among sexual and parthenogenetic lizards in the genus *Cnemidophorus* (Teiidae). *Journal of Experimental Zoology*, *171*, 175–183. https://doi.org/10.1002/jez.1401710205

Neaves, W. B., & Baumann, P. (2011). Unisexual reproduction among vertebrates. *Trends in Genetics*, *27*, 81–88. https://doi.org/10.1016/j.tig.2010.12.002

Otto, S. P., & Lenormand, T. (2002). Resolving the paradox of sex and recombination. *Nature Reviews Genetics*, *3*, 252–261. https://doi.org/10.1038/nrg761

Parker, E. D. Jr (1979). Ecological implications of clonal diversity in parthenogenetic morphospecies. *American Zoologist*, *19*, 753–762. https://doi.org/10.1093/icb/19.3.753

Parker, E. D. Jr, & Selander, R. K. (1976). The organization of genetic diversity in the parthenogenetic lizard *Cnemidophorus tesselatus*. *Genetics*, *84*, 791–805.

Parker, E. D. Jr, & Selander, R. K. (1984). Low clonal diversity in the parthenogenetic lizard *Cnemidophorus neomexicanus* (Sauria: Teiidae). *Herpetologica*, *40*, 245–252.

Patterson, N., Moorjani, P., Luo, Y., Mallick, S., Rohland, N., Zhan, Y., Genschoreck, T., Webster, T., & Reich, D. (2012). Ancient admixture in human history. *Genetics*, *192*, 1065–1093. https://doi.org/10.1534/genetics.112.145037

Paulissen, M. A. (1994). Microhabitat use and escape behaviors of syntopic clonal complexes of the parthenogenetic whiptail lizard *Cnemidophorus laredoensis*. *The American Midland Naturalist*, *132*, 10–18. https://doi.org/10.2307/2426196

Paulissen, M. A. (1999). Life History and drought tolerance of the parthenogenetic whiptail lizard *Cnemidophorus laredoensis* (Teiidae). *Herpetological Natural History*, *7*, 41–57.

Paulissen, M. A., Walker, J. M., & Cordes, J. E. (1988). Ecology of syntopic clones of the parthenogenetic whiptail lizard, *Cnemidophorus laredoensis*. *Journal of Herpetology*, *22*, 331–342. https://doi.org/10.2307/1564157

Paulissen, M. A., Walker, J. M., & Cordes, J. E. (2001). Status of the parthenogenetic lizards of the *Cnemidophorus laredoensis* complex in Texas: Re-survey after eleven years. *Texas Journal of Science*, *53*, 121–138.

Pritchard, J. K., Stephens, M., & Donnelly, P. (2000). Inference of population structure using multilocus genotype data. *Genetics*, *155*, 945–959. https://doi.org/10.1093/genetics/155.2.945

Rabeling, C., Gonzales, O., Schultz, T. R., Bacci, M., Garcia, M. V. B., Verhaagh, M., Ishak, H. D., & Mueller, U. G. (2011). Cryptic sexual populations account for genetic diversity and ecological success in a widely distributed, asexual fungus-growing ant. *Proceedings of the National Academy of Sciences of the United States of America*, *108*, 12366–12371. https://doi.org/10.1073/pnas.1105467108

Rambaut, A., Drummond, A. J., Xie, D., Baele, G., & Suchard, M. A. (2018). Posterior summarization in Bayesian phylogenetics using Tracer 1.7. *Systematic Biology*, *67*, 901–904. https://doi.org/10.1093/sysbio/syy032

Rochette, N. C., Rivera-Colón, A. G., & Catchen, J. M. (2019). Stacks 2: Analytical methods for paired-end sequencing improve RADseq-based population genomics. *Molecular Ecology*, *28*, 4737–4754. https://doi.org/10.1111/mec.15253

Ronquist, F., Teslenko, M., van der Mark, P., Ayres, D. L., Darling, A., Höhna, S., Larget, B., Liu, L., Suchard, M. A., & Huelsenbeck, J. (2012). MrBayes 3.2: Efficient Bayesian phylogenetic inference

and model choice across a large model space. *Systematic Biology*, *61*, 539–542.

Schön, I., Martens, K., & van Dijk, P. (Eds.) (2014). *Lost sex: The evolutionary biology of parthenogenesis*. Springer.

Schultz, R. J. (1973). Unisexual fish: Laboratory synthesis of a "species". *Science*, *179*, 180–181. https://doi.org/10.1126/science.179.4069.180

Schwander, T., & Crespi, B. J. (2009). Twigs on the tree of life? Neutral and selective models for integrating macroevolutionary patterns with microevolutionary processes in the analysis of asexuality. *Molecular Ecology*, *18*, 28–42. https://doi.org/10.1111/j.1365-294X.2008.03992.x

Sievert, L. M., & Paulissen, M. A. (1996). Temperature selection and thermoregulatory precision of bisexual and parthenogenetic *Cnemidophorus* lizards from southern Texas, USA. *Journal of Thermal Biology*, *21*, 15–20. https://doi.org/10.1016/0306-4565(95)00018-6

Spencer, C. C. A., Deloukas, P., Hunt, S., Mullikin, J., Myers, S., Silverman, B., Donnelly, P., Bentley, D., & McVean, G. (2006). The influence of recombination on human genetic diversity. *PLoS Genetics*, *2*, e148. https://doi.org/10.1371/journal.pgen.0020148

Stroud, J. T., Giery, S. T., Outerbridge, M., & Feeley, K. J. (2019). Ecological character displacement alters the outcome of priority effects during community assembly. *Ecology*, *100*, e02727. https://doi.org/10.1002/ecy.2727

Taylor, H. L., Cole, C. J., Manning, G. J., Cordes, J. E., & Walker, J. M. (2012). Comparative meristic variability in whiptail lizards (Teiidae, *Aspidoscelis*): Samples of parthenogenetic *A. tesselata* versus samples of sexually reproducing *A. sexlineata*, *A. marmorata*, and *A. gularis septemvittata*. *American Museum Novitates*, *3744*, 1–24.

Terhorst, J., & Song, Y. S. (2015). Fundamental limits on the accuracy of demographic inference based on the sample frequency spectrum. *Proceedings of the National Academy of Sciences of the United States of America*, *112*, 7677–7682. https://doi.org/10.1073/pnas.1503717112

Than, C., Ruths, D., & Nakhleh, L. (2008). PhyloNet: A software package for analyzing and reconstructing reticulate evolutionary relationships. *BMC Bioinformatics*, *9*, 322. https://doi.org/10.1186/1471-2105-9-322

Vitt, L. J. (2000). Ecological consequences of body size in neonatal and small-bodied lizards in the Neotropics. *Herpetological Monographs*, *14*, 388–400. https://doi.org/10.2307/1467053

Vrijenhoek, R. C. (1979). Factors affecting clonal diversity and coexistence. *American Zoologist*, *19*, 787–797. https://doi.org/10.1093/icb/19.3.787

Walker, J. M. (1987). Distribution and habitat of a new major clone of a parthenogenetic whiptail lizard (genus *Cnemidophorus*) in Texas and Mexico. *Texas Journal of Science*, *39*, 313–334.

Walker, J. M., Abuhteba, R. M., & Cordes, J. E. (1991). Morphological and experimental verification of hybridization between all-female *Cnemidophorus laredoensis* B and gonochoristic *Cnemidophorus gularis* (Squamata: Teiidae). *Herpetologica*, *47*, 152–164.

Walker, J. M., Cordes, J. E., & Paulissen, M. A. (1988). Hybrids of two parthenogenetic clonal complexes and a gonochoristic species of *Cnemidophorus* and the relationship of hybridization to habitat characteristics. *Journal of Herpetology*, *23*, 119–130. https://doi.org/10.2307/1564017

Walker, J. M., Cordes, J. E., & Paulissen, M. A. (2004). Characteristics of peripheral populations of parthenogenetic *Cnemidophorus laredoensis* A (Squamata: Teiidae), in southern Texas. *Texas Journal of Science*, *56*, 237–252.

Walker, J. M., Cordes, J. E., & Paulissen, M. A. (2016). Rare syntopy of the diploid parthenogenetic lizard (*Aspidoscelis laredoensis* B) and both gonochoristic progenitors (*A. gularis* and *A. sexlineata*) in Texas, USA. *Herpetological Conservation and Biology*, *11*, 29–39.

Walker, J. M., Guest, W. C., Cordes, J. E., & Paulissen, M. A. (1989). Morphological and chromosomal evidence of hybridization between all-female *Cnemidophorus laredoensis* and gonochoristic *Cnemidophorus gularis*. *Copeia*, *1989*, 1059–1064. https://doi.org/10.2307/1446000

Walker, J. M., Paulissen, M. A., & Cordes, J. E. (1996). Apparent changes in the composition of a community of Cnemidophorine lizards (Sauria: Teiidae) in a subtropical Texas forest. *The Southwestern Naturalist*, *41*, 64–67.

Walker, J. M., Taylor, H. L., Manning, G. J., Cordes, J. E., Montgomery, C. E., Livo, L. J., Keefer, S., & Loeffler, C. (2012). Michelle's lizard: identity, relationships, and ecological status of an array of parthenogenetic lizards (Genus *Aspidoscelis*: Squamata: Teiidae) in Colorado, USA. *Herpetological Conservation and Biology*, *7*, 227–248.

Warren, W. C., García-Pérez, R., Xu, S., Lampert, K. P., Chalopin, D., Stöck, M., Loewe, L., Lu, Y., Kuderna, L., Minx, P., Montague, M. J., Tomlinson, C., Hillier, L. D. W., Murphy, D. N., Wang, J., Wang, Z., Garcia, C. M., Thomas, G. C. W., Volff, J.-N., … Schartl, M. (2018). Clonal polymorphism and high heterozygosity in the celibate genome of the Amazon molly. *Nature Ecology and Evolution*, *2*, 669–679. https://doi.org/10.1038/s41559-018-0473-y.

Weir, B. S., & Cockerham, C. C. (1984). Estimating F-statistics for the analysis of population structure. *Evolution*, *38*, 1358–1370.

Weiß, C. L., Pais, M., Cano, L. M., Kamoun, S., & Burbano, H. A. (2018). nQuire: A statistical framework for ploidy estimation using next generation sequencing. *BMC Bioinformatics*, *19*, 122. https://doi.org/10.1186/s12859-018-2128-z

White, M. J. D. (1970). Heterozygosity and genetic polymorphism in parthenogenetic animals. *Essays in evolution and genetics in honor of theodosius dobzhansky* (pp. 237–262). Springer US.

Wright, J. W. (1993). Evolution of the lizards of the genus *Cnemidophorus*. In J. W. Wright, & L. J. Vitt (Eds.), *Biology of whiptail lizards (genus Cnemidophorus)* (pp. 27–81). Oklahoma Museum of Natural History.

Wright, J. W., & Lowe, C. H. (1968). Weeds, polyploids, parthenogenesis, and the geographical and ecological distribution of all-female species of *Cnemidophorus*. *Copeia*, *1968*, 128–138. https://doi.org/10.2307/1441559

Wright, J. W., Spolsky, C., & Brown, W. M. (1983). The origin of the parthenogenetic lizard *Cnemidophorus laredoensis* inferred from mitochondrial DNA analysis. *Herpetologica*, *39*, 410–416.

Zheng, X., Levine, D., Shen, J., Gogarten, S. M., Laurie, C., & Weir, B. S. (2012). A high-performance computing toolset for relatedness and principal component analysis of SNP data. *Bioinformatics*, *28*, 3326–3328. https://doi.org/10.1093/bioinformatics/bts606

Zhu, J., & Nakhleh, L. (2018). Inference of species phylogenies from bi-allelic markers using pseudo-likelihood. *Bioinformatics*, *34*, 376–385. https://doi.org/10.1093/bioinformatics/bty295

SUPPORTING INFORMATION

Additional supporting information may be found in the online version of the article at the publisher's website.

How to cite this article: Barley, A. J., Cordes, J. E., Walker, J. M., & Thomson, R. C. (2021). Genetic diversity and the origins of parthenogenesis in the teiid lizard *Aspidoscelis laredoensis*. *Molecular Ecology*, 00, 1–13. https://doi.org/10.1111/mec.16213